

Spectral barcoding of quantum dots: Deciphering structural motifs from the excitonic spectra

Vladan Mlinar and Alex Zunger*

National Renewable Energy Laboratory, Golden, Colorado 80401, USA

(Received 9 January 2009; revised manuscript received 6 May 2009; published 29 July 2009)

Self-assembled semiconductor quantum dots (QDs) show in high-resolution single-dot spectra a multitude of sharp lines, resembling a barcode, due to various neutral and charged exciton complexes. Here we propose the “spectral barcoding” method that deciphers structural motifs of dots by using such barcode as input to an artificial-intelligence learning system. Thus, we invert the common practice of deducing spectra from structure by deducing structure from spectra. This approach (i) lays the foundation for building a much needed structure-spectra understanding for large nanostructures and (ii) can guide future design of desired optical features of QDs by controlling during growth only those structural motifs that decide given optical features.

DOI: [10.1103/PhysRevB.80.035328](https://doi.org/10.1103/PhysRevB.80.035328)

PACS number(s): 73.21.La, 02.30.Zz, 68.65.-k, 78.67.-n

I. INTRODUCTION

The establishment of relationship between structure and spectra in molecules has historically been facilitated by the accumulated knowledge on electronic and vibrational spectral fingerprints of specific groups making up the molecules.^{1–5} Indeed, the relationship between these disciplines has propelled our understanding of the nature of the chemical bond^{3,4} and formed the basis for deliberate design of molecules with given properties.^{6,7} In recent years, nanostructures such as quantum dots (QDs), which can be grown deterministically and reproducibly by given and established synthesis protocols,⁸ have emerged as highly useful for observing intriguing physical effects resulting from interelectronic and spin interactions in confined spaces.^{9–12} However, unlike the case of discrete molecules and crystals, the position of each and every atom in the QD structure is often not known.^{13–15} Moreover, the association of vibrational or NMR fingerprints with specific molecular groups is currently not applicable to QD spectroscopy. Yet, at the heart of most conceived optical application of nanostructures (light emitting markers,¹⁶ single-photon sources,¹⁷ or solid-state lasers¹⁸) lays the ability to design required spectroscopic features via control of the grown structure. This paper addresses the important disconnect between spectra and structure for large (e.g., 10^5 atom) systems, by using the excitonic spectra as *input* to a learning system based on many-body pseudopotential calculations of spectra and obtaining as *output* some of the structural motifs of the system. We illustrate our method on (In,Ga)As/GaAs QDs but we will not use any specific features of this system except the existence of detailed spectroscopic data and virtually no atomic-scale structural information. Our method is thus applicable to any large system for which there is a detailed spectrum.

Self-assembled nanostructures are simple semiconductor “macromolecules” such as (In, Ga)As made of $\sim 10^4$ – 10^6 atoms, seamlessly embedded in another semiconductor matrix (e.g., GaAs).⁸ Currently available methods for structural characterization cannot resolve full atomic-scale structure but rather partial structural motifs such as shape, base size, height, and composition profile.^{13–15,19} At the same time, spectroscopy of self-assembled QDs now routinely reveal an amazingly rich set of very sharp excitonic lines in single-dot

emission spectrum [e.g., Fig. 1(a)].^{9–11,21} The structural perfectness (no impurities, dislocations, and defects), the ability to charge the system with a few electrons or holes, and the excellent isolation from the environment in self-assembled dots result in electronic spectra consisting of a series of 10–20 ultrasharp (μeV) lines, appearing in a narrow energy range of ~ 10 meV, unheard of in macromolecules of comparable molecular weight. We submit that such spectra must encode in it information on the structure. The physical basis of such a view is as follows: Fig. 1(a) shows typical measured single-dot spectra of a prototype self-assembled dot emitting around 1.3 eV. The spectroscopic transitions seen result from the recombination of an electron in the conduction band with a hole in the valence band, at the presence of additional N_e-1 spectator electrons and N_h-1 spectator holes occupying other electronic energy levels. The transitions shown in Fig. 1(a) include the neutral monoexciton X^0 [$(N_h=1; N_e=1)$]; the trion X^{-1} labeled (1, 2); the neutral biexciton XX^0 labeled (2, 2), the negatively charged biexcitons XX^{-1} (2, 3), etc. These are identified experimentally^{9–11} by tuning the direction and amplitude of electric field in which the dot is embedded. Whereas the low-resolution spectroscopic features seen on a broader energy scale of ~ 100 meV are often insensitive to structural details (e.g., showing spectral peaks that are common to different excitons, referred to as “hidden symmetry”^{22,23}), we will see that the sequences of multiexcitonic lines observed on ~ 10 meV scale, illustrated in Fig. 1(a), contain crucial information on the geometry and stoichiometry of the dot. This is so because excitonic lines are determined by the wave functions of the confined carriers and, in turn, the wave functions are controlled by the quantum confinement reflecting the structure and composition. The usual practice in quantum nanostructure theory^{9,10,24,25} is to use assumed structural characteristics as input and calculate the spectra on output. Here we attempt the *inverse problem*: use the excitonic spectra as input to determine the structure, where electronic structure theory provides the link. If such spectra-structure relationship emerges, it would help establish the presently missing structural basis for quantum-dot spectroscopy. For example, it might reveal which structural motifs control certain optical features and which optical features (e.g., sequence of certain emission lines) are insensitive to given structural features. Such relationships could be used to predict structural motifs

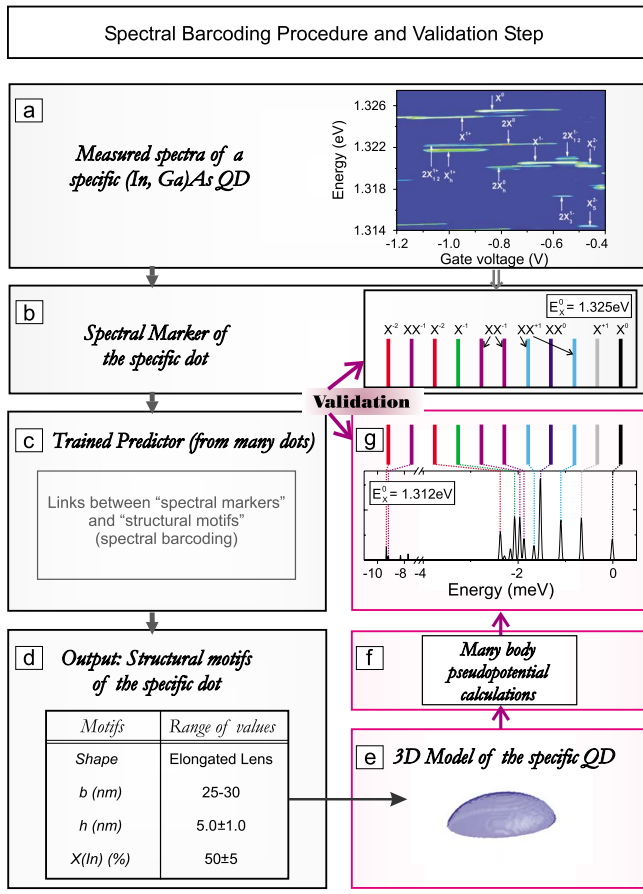


FIG. 1. (Color online) Spectral barcoding procedure and consistency test for a specific (In,Ga)As QD. (a) Illustrative measured spectrum of ~ 1.3 eV emitting MBE grown dot (Ref. 20). The exciton lines exhibit a Stark shift and the energy differences between the exciton lines have a small dependence on bias. The Stark shift does not change the ordering of the excitonic lines (Ref. 20). (b) Spectral marker is chosen to be a sequence of excitonic emission lines, representing it by equal length, straight lines distinguishable only by the given assignment and monoexciton energy. (c) Spectral barcoding procedure. (d) structural motifs deduced by the spectral barcoding procedure. (e) 3D QD structural model constructed using structural motifs (d), and (f) then used as input into the many-body pseudopotential method. (g) Calculated excitonic spectra and output spectral marker.

for a yet unknown spectral marker. Perhaps in the future, such an approach might open the possibilities of selectively controlling via growth specific structural motifs so as to achieve a desired, target spectral behavior of QDs. We are aware of similar attempts in molecular spectroscopy to use spectra and deduce structure. For example, in molecular chemistry, various forms of spectroscopy have been used to infer structure. Vibrational or NMR fingerprints have been associated with specific molecular groups using artificial-intelligence methods (see e.g., Refs. 5 and 7). However, currently available spectroscopy of self-assembled QDs consists of electronic spectra only and, furthermore, establishing links between molecular groups/structural motifs and spectral features is currently impossible in QD given that the actual position of the atoms within such large nanosystem

($\sim 10^4$ – 10^6 atoms) is not known. Therefore, our proposed approach is somewhat different from those historically used in chemistry.

II. SPECTRAL BARCODING PROCEDURE

A. Philosophy behind spectral barcoding

Whereas the full emission spectrum, consisting of all lines and their intensities can be viewed as the “QD DNA,” a partial spectral information from the spectra will be denoted here as the “QD spectral marker” or “spectral barcode.” Spectral marker can be chosen arbitrarily from the emission spectrum but such that it does not depend on uncontrollable variables as, e.g., atomic-scale randomness.²⁶ Here, we chose a subsequence of excitonic emission lines to be spectral-marker barcode, as shown in Fig. 1(b). There are different ways to select a subset. For example, we could use the sequence of lines, e.g., X^{-2} , X^{-1} , XX^0 , and X^0 ; this sequence of emission lines does not depend on the atomic-scale randomness, as illustrated in Appendix A. There are analogous partial structural constructs: the motifs can be defined as geometric shape, base size, height, average chemical composition, and composition profile. We propose the procedure we will term “spectral barcoding” to determine whether there exists a set of QD structural motifs which are correlated with specific spectral markers. It is likely that such relationship between spectral-barcode marker and structural motifs will be multivalued, i.e., there is a range of base size and heights that structural motifs can take and still produce the targeted spectral markers. However (i) this range is rather narrow [see, e.g., Sec. II C and Fig. 1(d)], (ii) the barcoding procedure eliminates an astronomic number of geometries that are in violation of the spectroscopic sequence. Finally, (iii) the existence of a few structural motifs that give the same spectral sequence is a fact that has to be reckoned with as inherent to the spectra-structure mapping. Actually, this fact can even be useful when it becomes necessary to design structures with given optical response. It is reassuring that a few structures can satisfy the requirements. We expect, in general, that the richer the input spectral-barcode marker, the more detailed will the output set of structural motifs be. However, even using a limited spectral information, it is important to learn which structural motifs are sensitive and which are not.

To deduce such structural motifs using spectroscopic features as input, we exploit a methodology used in biology.^{27,28} In DNA research, knowledge of the sequence of the entire DNA (genomics) uniquely decides the identity of the individual. However, restriction to partial information (a subsequence called genetic marker) affords identification of an individual as belonging to a broader class (species), without deciding its identity within the class.²⁸ Analogously, whereas the entire spectra of an individual QD might define its complete structure, a choice of a partial subsequence of lines (spectral marker), can identify a nanosystem as belonging to a group with common structural motifs. We expect, in general, that the richer the input spectral-barcode marker, the more detailed will the output set of structural motifs be. For example, we may find that specification of the energy of a

TABLE I. QD structure (S_i) discretized into a set of $N_s=5$ structural motifs, each taking up one of N_v possible values. QD base length and height are denoted as b and h , respectively. All dots are sitting on 2 ML wetting layer.

Value/structural motif	Shape	b (nm)	h (nm)	X_{In} (%)	In profile
Value 1	Truncated cone	12	2.0	50	Homogeneous
Value 2	Truncated pyramid	18	3.0	60	Linear
Value 3	Lens	20	3.5	70	
Value 4	Elongated lens in [100]	23	4.0	80	
Value 5	Elongated lens in [110]	25	5.0	90	
Value 6	Elongated lens in [$\bar{1}10$]	30	6.0	100	

monoexciton as a sole spectral marker of a given QD may define a combination of several structural motifs, all leading to that spectral marker, but that such spectral marker is insufficient to pin down the individual values of each of the structural motifs. One might expect that ultimately, the full “spectral DNA” (transition energies over a broad range, intensities, and line shapes) may be needed to establish much of the complete structure. We suggest, however, that for many purposes the knowledge of electronic structure-deciding (“principal”) structural motifs is both sufficient and important.

B. How does the spectral barcoding work?

To study the spectra \rightarrow structure link we use three ingredients. First, we use theory to predict the spectra for a given structure. Here we use an atomistic pseudopotential many-body method (see Appendix B), a state-of-the-art approach that includes the relevant single-body (band mixing and intervalley mixing) and many-body (direct Coulomb, exchange, and correlation energies) physical effects present in semiconductor QDs.^{9,29,30} This methodology was used previously to explain single-dot spectroscopy of charged QDs showing an excellent agreement with experiment.⁹ Second, we create a library of assumed structures, covering a wide range of possible structural motifs^{14,15} (Table I), and predict their multiexcitonic spectra via the theory noted above. Third, we use data reduction (machine learning) techniques^{31,32} to distill from the library the links between structural motifs and spectral markers. Once this is known, we are ready to predict the structural motifs of another measured or calculated spectra as input.

We test this concept on the widely studied⁸ self-assembled (In,Ga)As/GaAs QDs. Our library of structural motifs is created by discretizing the structural properties (S_i) into a set of N_s motifs, each taking up one of N_v possible values, as illustrated in Table I. This defines a library of different QDs (240 in our example). For each of these dots we solve the Schrödinger equations using pseudopotential many-body theory^{29,30} obtaining the multiexcitonic emission lines for each structure. This structure vs spectra library establishes deterministic links between each structure and its spectral marker (=the sequence of emission lines). We next data mine the library by using the Bayesian data reduction algorithm

(BDRA).³¹ BDRA training consists of testing how each structural motif and its corresponding values (Table I) influences the spectral marker, allowing the possibility that structural motifs are correlated. As a result, BDRA identifies the set of structural motifs that are responsible for a given spectral-barcode sequence. BDRA training applied to different spectral-barcode markers reveals which structural motifs tend to emerge together for a given spectral-barcode marker.

C. Consistency test

Since we do not have an experimental determination of an (In, Ga)As QD structure (so comparison with experiment is currently impossible), we design a nontrivial internal consistency test as follows. We start from the measured emission spectra¹¹ of a typical ~ 1.3 eV dot shown in Fig. 1(a). We next represent the spectra as a spectral barcode [Fig. 1(b)]. Inserting this spectral barcode into the previously trained predictor [Fig. 1(c)], we deduce a set of structural motifs, summarized in Fig. 1(d), that according to our data reduction study explain the input spectral marker of *this particular dot*. We see that these structural motifs span some range. All structures within this range give the correct barcode. In other words, the limited spectral barcode used, says this specific dot has a basis size between 25 and 30 nm, height between 4 and 6 nm, and In composition between 45% and 55%. The sensitivity of spectral marker to these structural motifs is however, rather strong. We then use such motifs to assemble a three-dimensional (3D) QD structural model [Fig. 1(e)], consistent with the set of identified structural motifs (a few such structures can be constructed). To verify the method, we then input this 3D QD structure into a fresh calculation of the excitonic spectra, using the pseudopotential many-body method^{29,30} [Fig. 1(f)]. The output of this spectral calculation is shown in Fig. 1(g), where it is compared with the original input barcode of Fig. 1(b). We see that this approach is able to reproduce, with no exception the input spectral sequence of all spectroscopic multiexciton emission lines. This is the case for all 3D structures assembled from the motifs in Fig. 1(d). This is nontrivial. Indeed, using our library of 240 QDs (out of possible $6^4=2592$ different QD structures), the spectral barcoding method is able to deduce the structural motifs which lead to one targeted sequence of multiexciton emission lines (given relative to the monoexciton energy) out of

1 663 200 possibilities. We note that achieving the correct multiexcitonic barcode sequence is nontrivial not only in terms of the large number of possible combinations but also because it requires knowing rather accurately the electron and hole wave functions. The spectral barcoding method does not rely on any specific QD feature or the (In,Ga)As system, in particular, except requiring sufficient spectroscopic data (~ 10 emission lines). Clearly, this currently limits the application of the method to cases where such rich spectra exist. However, future prospects of high resolution in single-molecule spectroscopy seem limitless.

III. IMPLICATIONS OF THE SPECTRAL BARCODING PROCEDURE

A. Structural information revealed in stages

The general utility of the barcoding approach becomes obvious when one inspects the gradual emergence of specific spectra-structure links. Indeed, much like peeling an onion, the structural information is revealed in stages, reflecting the level of detail provided as input by the spectral marker. For example,

(i) If we use only the energy E_X^0 of the monoexciton as the sole spectral marker, numerous combinations of the structural properties from Table I give the same result. For example, denoting by h and b the QD height and base length, respectively, and assuming a homogeneous In profile with composition \bar{X}_{In} , a monoexciton with energy $E_X^0 = 1.305 \pm 0.010$ eV can be obtained either by a lens-shaped dot with $h=3.5$ nm, $b=15$ nm, and $\bar{X}_{\text{In}}=60\%$, or by a truncated cone dot with $h=2.0$ nm, $b=20$ nm, and $\bar{X}_{\text{In}}=60\%$, or by an elongated lens dot with $h=4.0$ nm, $b=25$ nm, and $\bar{X}_{\text{In}}=50\%$.

(ii) If we enrich the spectral-barcode information by requiring it to satisfy certain sequence of multiexcitonic lines, further detail on the structural motifs emerge. While experimentally one observes some spectroscopic dot-to-dot variations, remarkably^{9,11} all molecular-beam epitaxy (MBE) grown (In,Ga)As/GaAs QDs appear to manifest spectroscopically the same hard rules (HR) as follows: (HR1) the energies of the X^{-1} , XX^0 , X_S^{-2} , and X_T^{-2} lines are always redshifted relative to X^0 . (HR2) the XX^0 line always lies between X^0 and X^{-1} , and (HR3) the X_T^{-2} line is always redshifted relative to X^{-1} . Whereas any sequence of excitonic lines could be “inverted” by the learning machine to distil structural motifs, we chose here to seek the structural motifs responsible for three spectroscopic hard rules akin universally to all MBE grown (In,Ga)As/GaAs QDs. We will refer to these as HR-derived “primary structural motifs.” The BDRA data mining procedure identifies base lengths, heights, and average indium composition \bar{X}_{In} as HR-derived primary structural motifs, i.e., as those that control the hard rules. The remaining structural motifs are irrelevant (i.e., not primary) as far as controlling three HRs is concerned. For example, perhaps surprisingly it turns out that shape (viz., Table I) is not a primary motif. Figure 2 shows the range of primary structural motifs values that lead to satisfaction of

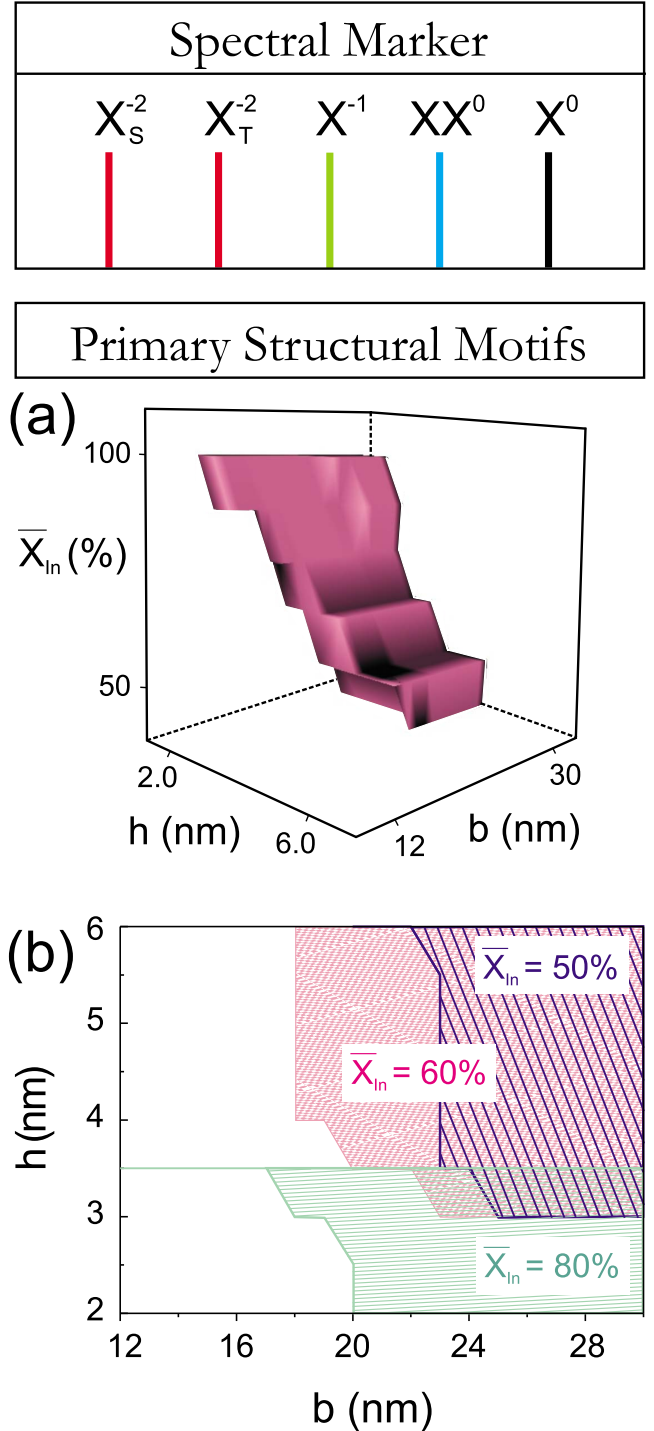


FIG. 2. (Color online) Primary structural motifs underlying the spectral hard rules. (a) The range of primary structural motifs heights (h), base lengths (b), and average In composition (\bar{X}_{In}) that lead to satisfaction of the spectral HRs. (b) Allowed b and h for \bar{X}_{In} taking values of 50%, 60%, and 80%.

spectral HRs. The establishment of clear links between the spectroscopic hard rules and the primary structural motifs shows that the latter are not random variables. For example, for a given \bar{X}_{In} , the excitonic spectra suggests that MBE grown QDs have a restricted and correlated range of base

lengths and heights [Fig. 2(b)]. Hence, either the growth kinetics of MBE QDs imposes these limitations or emission from the dots with primary motifs outside shaded regions in Figs. 2(a) and 2(b) is weak.

(iii) If we enrich the spectral-barcode marker by constraining it to satisfy the sequence of 11 excitonic lines [Fig. 1(b)] we obtain a narrower range of base lengths and heights, and the requirement for a particular shape now arises [see Fig. 1(d)]. Having trained the structure-spectra learning machine to decipher the structural content of the spectral barcode determining the HR, the BDRA is next applied to the remaining excitonic sequence, searching for secondary structural motifs that determine: (a) the position of X^{+1} relative to X^0 (allowing two possibilities X^{+1} redshifted relative to X^0 and X^{+1} blueshifted relative to X^0), (b) the position of three lines of XX^{-1} (XX^{+1}) relative to the sequence of emission lines that obey the HR, and (c) XX^{-1} (XX^{+1}) relative to X^{+1} . We thus find the structural motifs and the range of values each of them can take [Fig. 1(d)]. For example, it turns out that shape as a nonprimary motif, correlated with the primary ones, determines the sequence of X^{+1} , XX^{-1} , and XX^{+1} emission lines.

The insights revealed can find applications in analysis of structural characterization methods.^{14,15} For example, cross-sectional scanning tunneling microscopy (XSTM) measurements alone often are insufficient to narrow down the structure so such measurements were previously augmented by some optical data (e.g., by the optically measured exciton energy E_X^0 to determine a compositional profile of a quantum well³³). However, as our analysis shows, the monoexciton energy as spectral marker cannot pin down the individual values of the structural motifs. Our method offers far more detailed, spectroscopically derived structural motifs that can more effectively augment such XSTM measurements, which still remains to be verified experimentally.

B. Toward achieving desired spectroscopic features

By tracking the link between spectral marker and structural motifs we open the possibilities for achieving desired spectroscopic features by controlling during the growth just the relevant structural motifs (not the positions of all atoms) so as to achieve a desired optical behavior of nanostructures. For example, Fig. 3 shows the variation in the sequence of the emission lines with the QD height and base length for the fixed indium composition $\bar{X}_{In}=70\%$. We are able to identify three regions, denoted as α , β , and γ in Fig. 3, depending on the sequence of emission lines. Note that only the range of base lengths and heights belonging to the region β satisfies spectral HRs characteristic for MBE grown QDs. We here predict that if one could have a dot with structural properties corresponding to region α or γ then a new sequence of HR-violating lines would emerge. The association of a combination of specific structural motifs with a target spectral marker implies that two QDs need not have identical 3D structures to give identical optical response. All they need to have in common are the relevant structural motifs.

C. Different growth modes intrinsically lead to limited range of QD sizes and compositions?

Although we illustrated the extraction of structural motifs for MBE grown QDs in Sec. II C, our spectral barcoding

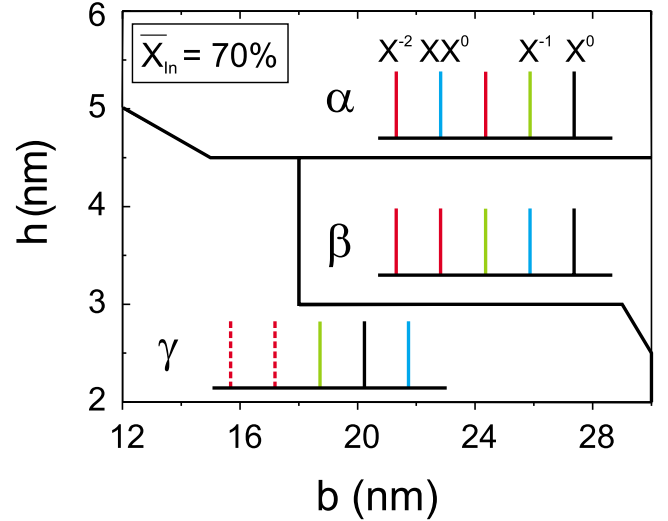


FIG. 3. (Color online) Variation in the sequence of emission lines which obey HRs (denoted as α , β , and γ) as a function of h and b for $\bar{X}_{In}=70\%$. X^{-2} emission lines are shown by dashed lines because there is only one confined electron level for QDs (X^{-2} does not exist) with $b \leq 15$ nm and $h \leq 4$ nm.

procedure is not limited only to this growth mode. Figure 3 shows variation in sequence of HRs with height and base length for fixed $\bar{X}_{In}=70\%$. We see that for certain range of QD sizes (barcode γ in Fig. 3), the XX^0 line is blueshifted relative to X^0 , as is the case for dots grown by another widely used growth procedure metal-organic chemical-vapor deposition (MOCVD) with $E_X^0=1.25-1.35$ eV.³⁴ Figure 3 reveals that such MOCVD dots must have heights $2 \leq h \leq 4$ for the base lengths $12 \leq b < 18$, whereas for larger base lengths ($18 \leq b \leq 30$), the heights of MOCVD grown dots are $2 \leq h \leq 3$, i.e., smaller than those of MBE grown dots ($3 < h < 5$) for the same base lengths range. Furthermore, Rodt *et al.*³⁴ measured and analyzed cathodoluminescence spectroscopy data recorded on a large number of individual MOCVD grown QDs. Interestingly, all QDs with monoexciton energy in the range $E_X^0=1.25-1.35$ eV have the following sequence of the emission lines in the excitonic spectra: $X^{-1} < X^0 < XX^0 < XX^{+1} < X^{+1}$. Using this sequence as an input to the spectral barcoding procedure, we deduce following range of structural motifs for such MOCVD QDs: $\bar{X}_{In}=60-70\%$ and base length-height dependence is shown in Fig. 3. Note that using this sequence of emission lines as an input cannot distinguish between circular vs square vs elongated base.

Interestingly, Rodt *et al.*³⁴ do not report the existence of X^{-2} and XX^{-1} emission lines commonly seen in the spectra of MBE grown QDs.⁹⁻¹¹ This fact may suggest that these MOCVD grown QDs are rather flat with only one confined electron level in the dot. However, detailed spectroscopic study of these MOCVD dots is needed so to get more reliable structural information.

IV. SUMMARY

We proposed the spectral barcoding procedure to decipher structural motifs of QDs by using the segments of the elec-

tronic spectra (spectral marker) as input to the artificial-intelligence learning system (Bayesian data reduction algorithm). By tracking the link between spectral marker and structural motif (i) we establish the missing structural basis for QD spectroscopy, creating a beginning of a dictionary of spectral features vs structural motifs and (ii) provide guidelines for the design of desired optical features of QDs by controlling during growth simple structural motifs, rather than via attempts to control the complete structure of these large nanosystems.

ACKNOWLEDGMENTS

The authors thank P. A. Dalgarno and R. J. Warburton for their permission to reproduce measured emission spectra in Fig. 1(a) and R. J. Warburton for discussions and comments on the paper. This work was funded by the U.S. Department of Energy, Office of Science under NREL Contract No. DE-AC36-08GO28308.

APPENDIX A: ROLE OF ATOMIC-SCALE RANDOMNESS

(In,Ga)As QDs are usually alloyed, as revealed by structural characterization techniques.¹⁴ The fact QDs are alloyed, $\text{In}_x\text{Ga}_{1-x}$, implies there is a set of possible spatial configurations,³⁵ σ , and each can have distinct property $P(\sigma)$.³⁶ What particular spatial configuration σ each dot from an ensemble will have is unknown and cannot be controlled. We have already discussed in Ref. 36 how different random realizations (RRs) influence emission lines of several multiexcitonic transitions. Here we illustrate how different RRs influence distances between emission lines but not the sequence of lines on the example of X^{-2} and XX^{-1} transitions. Our results are shown in Fig. 4 for a flat low-In dot [base length 25 nm, height 2 nm, and $\bar{X}_{\text{In}}=60\%$].

APPENDIX B: MANY BODY PSEUDOPOTENTIAL CALCULATIONS

For the assumed size, shape, and composition of a QD we first relax the atomic position $\{\mathbf{R}_{i,\alpha}\}$ via the valence force

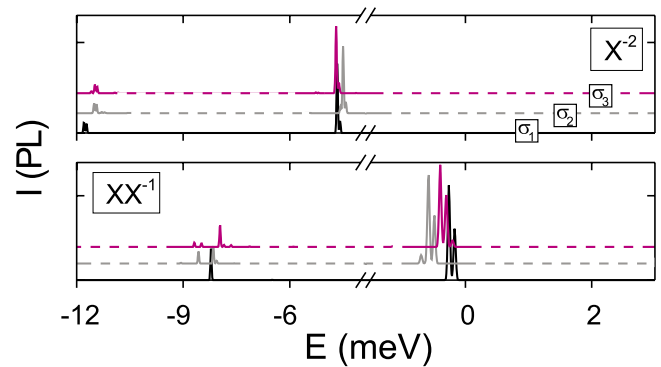


FIG. 4. (Color online). Influence of RR on the emission lines of the X^{-2} and XX^{-1} multiexcitonic transitions.

field method,³⁷ and construct the total pseudopotential of the system $V(\mathbf{r})$ by superposing the atomic (pseudo)potentials centered at the atomic equilibrium positions for $\sim 2 \times 10^6$ atoms, and adding the nonlocal spin-orbit V_{so} interaction, $V(\mathbf{r}) = V_{\text{so}} + \sum_{i,\alpha} v_{i,\alpha}(\mathbf{r} - \mathbf{R}_{i,\alpha})$. The Hamiltonian $-1/2\nabla^2 + V(\mathbf{r})$ is diagonalized in a basis $\{\phi_{n,\epsilon,\lambda}(\mathbf{k})\}$ of Bloch bands, of band index n , and wave vector \mathbf{k} for material λ (InAs, GaAs).²⁹ Multiexciton complexes are calculated using the configuration-interaction (CI) method.³⁰ Slater determinants are constructed from s , p , and d electron and hole orbitals (well separated in energy from remaining dot-confined states), which give 12 electron and 12 hole single-particle states (counting spin). No symmetry constraints are imposed to these basis states. Coulomb and exchange integrals are computed numerically from the pseudopotential single-particle orbitals. The screening function for these integrals contains an ionic and an electronic component that exhibit a smooth transition from unscreened at short range to screened at long range. Emission spectra is calculated using Fermi's golden rule applied to CI states, where configuration mixing in the initial and final states are reflected through variation in energetic positions and intensities of the emission lines.

*alex.zunger@nrel.gov

¹G. M. Barrow, *Introduction to Molecular Spectroscopy* (McGraw-Hill, New York, 1962).

²A. F. Wells, *Structural Inorganic Chemistry* (Clarendon, Oxford, UK, 1975).

³L. Pauling, *The Nature of the Chemical Bond and the Structure of Molecules and Crystals: An Introduction to Modern Structural Chemistry* (Cornell University Press, Ithaca, 1980).

⁴R. Hoffmann, *Solids and Surfaces: Chemist's View of Bonding in Extended Structures* (Wiley-VHC, New York, 1989).

⁵M. Peris, *Crit. Rev. Anal. Chem.* **26**, 219 (1996).

⁶M. Wang, X. Hu, D. N. Beratan, and W. Yang, *J. Am. Chem. Soc.* **128**, 3228 (2006).

⁷L. V. Gribov, *J. Mol. Struct.* **113**, 11 (1984).

⁸V. Shchukin, N. N. Ledentsov, and D. Bimberg, *Epitaxy of*

Nanostructures, Nanoscience and Technology (Springer, New York, 2003).

⁹M. Ediger, G. Bester, A. Badolato, P. M. Petroff, K. Karrai, A. Zunger, and R. J. Warburton, *Nat. Phys.* **3**, 774 (2007).

¹⁰M. Ediger, G. Bester, B. D. Gerardot, A. Badolato, P. M. Petroff, K. Karrai, A. Zunger, and R. J. Warburton, *Phys. Rev. Lett.* **98**, 036808 (2007).

¹¹P. A. Dalgarno, J. M. Smith, J. McFarlane, B. D. Gerardot, K. Karrai, A. Badolato, P. M. Petroff, and R. J. Warburton, *Phys. Rev. B* **77**, 245311 (2008).

¹²R. Hanson and D. D. Awschalom, *Nature (London)* **453**, 1043 (2008).

¹³S. I. Molina, A. M. Sánchez, A. M. Beltrán, D. L. Sales, T. Ben, M. F. Chisholm, M. Varela, S. J. Pennycook, P. L. Galindo, A. Papworth, P. J. Goodhew, and J. M. Ripalda, *Appl. Phys. Lett.*

- 91**, 263105 (2007).
- ¹⁴J. Stangl, V. Holý, and G. Bauer, *Rev. Mod. Phys.* **76**, 725 (2004).
- ¹⁵M. Bruls, J. W. A. M. Vugs, P. M. Koenraad, H. W. M. Salemnik, J. H. Wolter, M. Hopkinson, M. S. Skolnick, F. Long, and S. P. A. Gill, *Appl. Phys. Lett.* **81**, 1708 (2002).
- ¹⁶T. J. Fountaine, S. M. Wincovitch, D. H. Geho, S. Garfield, and S. Pittaluga, *Mod. Pathol.* **19**, 1181 (2006).
- ¹⁷M. Pelton, C. Santori, J. Vuckovic, B. Zhang, G. S. Solomon, J. Plant, and Y. Yamamoto, *Phys. Rev. Lett.* **89**, 233602 (2002).
- ¹⁸N. Kirstaedter, N. N. Ledentsov, M. Grundmann, D. Bimberg, V. Ustinov, S. Ruvimov, M. Maximov, P. Kop'ev, and Zh. Alferov, *Electron. Lett.* **30**, 1416 (1994).
- ¹⁹Disappointingly, methods for structural characterization are still not accurate enough to reveal the full atomic-scale structure. For example, one of the leading characterization methods, XSTM requires as input a good guess for the shape and composition profile of the dot where the ensuing structural determination is then performed and validated only within a neighborhood of such guesses (Ref. 15). Similar situation is with x-ray diffraction (Ref. 14) where the intensity distributions in the reciprocal space are recorded. From these reciprocal maps using initial guesses of QD shape and composition profile, and performing strain calculations, the final chemical composition profile is extracted. Also, transmission electron microscopy-based techniques are currently unable to go beyond qualitative description of QD compositional profile (Ref. 13).
- ²⁰P. A. Dalgarno and R. J. Warburton, private communication (September 2008).
- ²¹E. Poem, J. Shemesh, I. Marderfeld, D. Galushko, N. Akopian, D. Gershoni, B. D. Gerardot, A. Badolato, and P. M. Petroff, *Phys. Rev. B* **76**, 235304 (2007).
- ²²M. Bayer, O. Stern, P. Hawrylak, S. Fafard, and A. Forchel, *Nature (London)* **405**, 923 (2000).
- ²³V. Mlinar, A. Franceschetti, and A. Zunger, *Phys. Rev. B* **79**, 121307(R) (2009).
- ²⁴A. Zunger, *Mater. Res. Bull.* **23**, 35 (1998).
- ²⁵L. He, G. Bester, and A. Zunger, *Phys. Rev. Lett.* **94**, 016801 (2005).
- ²⁶Naturally, we will not select as relevant spectral-barcode features those aspects of the spectra that are altered by using different atomic-scale randomness. For example, a dot made of GaAs + InAs can manifest different configurations of Ga/In on cation sites for the fixed geometry and composition but calculations reveal that the splitting of a given (N_h, N_e) exciton into sub-meV fine structure is changed by such random realizations and thus will not be used to decide structure.
- ²⁷R. Lahaye, M. Van der Bank, D. Bogarin, J. Warner, F. Pupulin, G. Gigot, O. Maurin, S. Duthoit, T. G. Barraclough, and V. Savolainen, *Proc. Natl. Acad. Sci. U.S.A.* **105**, 2923 (2008).
- ²⁸W. J. Kress and D. L. Erickson, *Proc. Natl. Acad. Sci. U.S.A.* **105**, 2761 (2008).
- ²⁹L. W. Wang and A. Zunger, *Phys. Rev. B* **59**, 15806 (1999).
- ³⁰A. Franceschetti, H. Fu, L.-W. Wang, and A. Zunger, *Phys. Rev. B* **60**, 1819 (1999).
- ³¹R. S. Lynch, Jr. and P. K. Willett, *IEEE Trans. Syst., Man, Cybern., Part B: Cybern.* **33**, 448 (2003).
- ³²R. S. Lynch, Jr. and P. K. Willett, 2004 IEEE International Conference on Systems, Man, and Cybernetics, 2004, Vol. 2, p. 1336.
- ³³H. Chen, H. A. McKay, R. M. Feenstra, G. C. Aers, P. J. Poole, R. L. Williams, S. Charbonneau, P. G. Piva, T. W. Simpson, and I. V. Mitchell, *J. Appl. Phys.* **89**, 4815 (2001).
- ³⁴S. Rodt, A. Schliwa, K. Pötschke, F. Guffarth, and D. Bimberg, *Phys. Rev. B* **71**, 155325 (2005).
- ³⁵A configuration σ is defined as a particular occupation of each of the N lattice sites by either In or Ga atom.
- ³⁶V. Mlinar and A. Zunger, *Phys. Rev. B* **79**, 115416 (2009).
- ³⁷P. N. Keating, *Phys. Rev.* **145**, 637 (1966).